Sequential-Quadratic-Hamiltonian Optimal Control of Epidemic Models With an Arbitrary Number of Infected and Non-Infected Compartments

Francesca Calà Campana, Rami Katz, and Giulia Giordano, *Senior Member, IEEE*

***Abstract*—For a general class of epidemiological models with an arbitrary number of infected and non-infected compartments, we formulate an optimal vaccination control problem to minimize the number of infections and the cost of vaccination. We show that the problem can be solved efficiently with the sequential quadratic Hamiltonian (SQH) scheme, which we apply to the optimal control of epidemics for the first time and for which we prove rigorous global convergence guarantees in the case of a smooth cost functional. Our numerical simulations show that SQH outperforms the current state-of-the-art numerical scheme in mathematical epidemiology: its convergence can be guaranteed regardless of the initialization, it is faster and it is also applicable when the cost functional is non-smooth.**

***Index Terms*—Epidemic model, vaccination, optimal control, Pontryagin minimum principle.**

I. Introduction

MATHEMATICAL models have supported the analysis and the control of epidemics [1], [2], [3], [4], [5] since the introduction of the seminal SIR model [6], which considers three stages of infection: susceptible, infected and recovered. SIR-like mean-field compartmental models, describing the spread of an infectious disease in a large, well-mixed population, have been developed by adding increasingly more compartments, aimed at capturing the evolution of specific diseases with different infected (e.g., distinguishing between exposed but not yet infectious individuals, asymptomatic and symptomatic, undetected, diagnosed, quarantined) and non-infected (e.g., susceptible, recovered, vaccinated) categories, with several recent developments during the COVID-19 pandemic [7], [8], [9], [10], [11]. Optimal control theory is a powerful tool to design interventions aimed at curbing the contagion [12], [13], [14], [15], [16], [17].

Manuscript received 4 March 2024; revised 18 May 2024; accepted 1 June 2024. Date of publication 11 June 2024; date of current version 9 July 2024. This work was supported in part by the European Union through the ERC INSPIRE Grant under Project 101076926, and in part by the NextGenerationEU, PRIN-22 Project PRIDE under Grant 2022LP77J4. Recommended by Senior Editor M. E. Valcher. *(Corresponding author: Giulia Giordano.)*

The authors are with the Department of Industrial Engineering, University of Trento, 38122 Trento, Italy (e-mail: f.calacampana@unitn.it; ramkatsee@gmail.com; giulia.giordano@unitn.it).

Digital Object Identifier 10.1109/LCSYS.2024.3412775

Here, to formulate an optimal epidemic control problem so that our results can have the broadest possible scope and validity, we consider a very general class of epidemiological models (Section II), similar to that in [18], with an arbitrary number of infected and non-infected compartments, which can seamlessly include vaccination, as well as waning immunity and the possibility of (re)infection for both recovered and vaccinated. In Section III, we formulate and analyze an optimal vaccination control problem aimed at minimizing the fraction of infected and the cost of vaccine rollout. We prove the existence of a solution and we derive the related optimality system in the Pontryagin-minimum-principle framework. Then, we propose to numerically solve the problem by using the sequential quadratic Hamiltonian (SQH) method [19], [20], [21], [22], recently developed to solve both smooth and non-smooth optimal control problems. We apply the SQH method to epidemiological control problems for the first time, and we prove global convergence guarantees for SQH that hold for the whole considered class of systems, with smooth cost functionals. As shown in Section IV, the proposed methodology outperforms the state-of-the-art forward-backward sweep (FBS) method used to solve optimal control problems in epidemiology and systems biology [12], [23], which is known to suffer from convergence issues [23], [24]. Differently from FBS, the SQH method can also be applied with non-smooth cost functionals. In our numerical experiments, we consider an extension of the SIDARTHE-V model [9], to demonstrate that the approach can easily handle complex and large-scale dynamics; a full version of our work that includes a richer set of examples and numerical simulations is available online [25].

II. The Class of Epidemic Models

We consider a class of compartmental models of the form

$$\begin{cases} \dot{x}(t) = Fx(t) + b\, w(t)^\top Cx(t) \\ \dot{w}(t) = Gw(t) - \mathrm{diag}(Cx(t))w(t) + Dx(t) + a \end{cases} \tag{1}$$

where $x(t),\, b \in \mathbb{R}^{n_1}_{\geq 0}$, $w(t),\, a \in \mathbb{R}^{n_2}_{\geq 0}$. The variables $\{x_i(t)\}_{i=1}^{n_1}$ represent the population fractions in different infected compartments, while the variables $\{w_i(t)\}_{i=1}^{n_2}$ represent the population fractions in non-infected (e.g., susceptible, recovered, vaccinated) compartments.

Matrices $F \in \mathbb{R}^{n_1 \times n_1}$, describing the flows among infected compartments along with recovery, and $G \in \mathbb{R}^{n_2 \times n_2}$, which

contains parameters related to vaccination and waning of immunity that drive the flows among non-infected compartments, are both Metzler and Hurwitz. The infection matrix $C \in \mathbb{R}^{n_2 \times n_1}_{\geq 0}$ includes the contagion parameters, while $D \in \mathbb{R}^{n_2 \times n_1}_{\geq 0}$ includes the recovery parameters. Vector a represents natality in the population, while F and G also include mortality rates. When formulating an epidemic control problem, the control parameters can be included in $G = G(u)$, when planning a vaccination campaign, or in $C = C(u)$, when planning non-pharmaceutical interventions (e.g., physical distancing, use of protective equipment, mobility restrictions). The total population is assumed constant over a finite time horizon $T > 0$ (meaning that natality and mortality compensate for each other): for all $t \in [0, T]$, $\sum_{i=1}^{n_1} x_i(t) + \sum_{j=1}^{n_2} w_j(t) = 1$. This implicitly enforces appropriate assumptions on the system matrices. Subject to these assumptions, the initial value problem (1) with initial conditions $x(0) = x_0$ and $w(0) = w_0$, such that $\sum_{i=1}^{n_1} x_{0,i} + \sum_{j=1}^{n_2} w_{0,j} = 1$, is well-posed and admits a unique solution $(x(t), w(t))$. The system is positive: if $x_0, w_0 \geq 0$, then $x(t), w(t) \geq 0$ for all $t \geq 0$.

The model (1) admits a disease-free equilibrium $(0, \bar{w})$, with $\bar{w}_i \geq 0$ and at least one $\bar{w}_j > 0$, $i, j = 1, \ldots, n_2$, to which we want to drive our system.

We can define the control reproduction number [18] as $\mathcal{R}_c \doteq \lambda(-b\bar{w}^\top C F^{-1})$, where $\lambda(\cdot)$ is the matrix spectral radius. In the absence of control, $\mathcal{R}_c$ is the basic reproduction number. The disease-free equilibrium is locally asymptotically stable if $\mathcal{R}_c < 1$ and unstable if $\mathcal{R}_c > 1$.

Example 1 (Extended SIDARTHE-V Model): In the model in [9], with five infected compartments (I, D, A, R, T), we introduce waning immunity with rates σ_i and (re)infection probabilities $\theta_i \in [0, 1]$ for recovered and vaccinated, as well as a birth rate ψ and non-COVID-related mortality rates μ_i, and we denote by u the vaccination rate:

$$\begin{cases} \dot{S} &= \psi - S(\alpha I + \beta D + \gamma A + \delta R) - uS + \sigma_1 H + \sigma_2 V - \mu_S S \\ \dot{I} &= S(\alpha I + \beta D + \gamma A + \delta R) - (\varepsilon + \zeta + \lambda) I + \theta_1 \alpha H I \\ &\quad + \theta_2 \alpha V I + \theta_3 \beta H D + \theta_4 \beta V D + \theta_5 \gamma H A + \theta_6 \gamma V A \\ &\quad + \theta_7 \delta H R + \theta_8 \delta V R - \mu_I I \\ \dot{D} &= \varepsilon I - (\eta + \rho) D - \mu_D D \\ \dot{A} &= \zeta I - (\theta + \mu + \kappa) A - \mu_A A \\ \dot{R} &= \eta D + \theta A - (\nu + \xi + \tau_1) R - \mu_R R \\ \dot{T} &= \mu A + \nu R - (\sigma + \tau_2) T - \mu_T T \\ \dot{H} &= \lambda I + \rho D + \kappa A + \xi R + \sigma T - \sigma_1 H - \theta_1 \alpha H I \\ &\quad - \theta_3 \beta H D - \theta_5 \gamma H A - \theta_7 \delta H R - \mu_H H \\ \dot{E} &= \tau_1 R + \tau_2 T \\ \dot{V} &= uS - \sigma_2 V - \theta_2 \alpha V I - \theta_4 \beta V D - \theta_6 \gamma V A - \theta_8 \delta V R - \mu_V V \end{cases}$$

The parameters α, β, γ and δ denote transmission rates; ε and θ diagnosis rates; ζ and η symptom onset rates; μ and ν aggravation rates; τ_1 and τ_2 COVID-related mortality rates; λ, κ, ξ, ρ and σ recovery rates. The system can be written as in (1) with $x = [I\ D\ A\ R\ T]^\top$, where I denotes asymptomatic undetected infected, D asymptomatic diagnosed infected, A symptomatic undetected infected, R symptomatic diagnosed infected, T diagnosed infected with life-threatening symptoms, and $w = [S\ H\ E\ V]^\top$, where S denotes susceptible, H recovered, E deceased, and V vaccinated individuals, by taking $F = \begin{bmatrix} -(\varepsilon+\zeta+\lambda+\mu_I) & 0 & 0 & 0 & 0 \\ \varepsilon & -(\eta+\rho+\mu_D) & 0 & 0 & 0 \\ \zeta & 0 & -(\theta+\mu+\kappa+\mu_A) & 0 & 0 \\ 0 & \eta & \theta & -(\nu+\xi+\tau_1+\mu_R) & 0 \\ 0 & 0 & \mu & \nu & -(\sigma+\tau_2+\mu_T) \end{bmatrix}$, $C = \begin{bmatrix} \alpha & \beta & \gamma & \delta & 0 \\ \theta_1\alpha & \theta_3\beta & \theta_5\gamma & \theta_7\delta & 0 \\ 0 & 0 & 0 & 0 & 0 \\ \theta_2\alpha & \theta_4\beta & \theta_6\gamma & \theta_8\delta & 0 \end{bmatrix}$, $D = \begin{bmatrix} 0 & 0 & 0 & 0 & 0 \\ \lambda & \rho & \kappa & \xi & \sigma \\ 0 & 0 & 0 & \tau_1 & \tau_2 \\ 0 & 0 & 0 & 0 & 0 \end{bmatrix}$, $G = \begin{bmatrix} -u - \mu_S & \sigma_1 & 0 & \sigma_2 \\ 0 & -\sigma_1 - \mu_H & 0 & 0 \\ 0 & 0 & 0 & 0 \\ u & 0 & 0 & -\sigma_2 - \mu_V \end{bmatrix}$, $a = [\psi\ 0\ 0\ 0\ 0]^\top$, $b = [1\ 0\ 0\ 0\ 0]^\top$. The disease-free equilibrium is $[\frac{\psi(\sigma_2+\mu_V)}{u\mu_V+\sigma_2\mu_S+\mu_S\mu_V}\ 0\ 0\ 0\ 0\ 0\ \bar{E}\ \frac{\psi u}{u\mu_V+\sigma_2\mu_S+\mu_S\mu_V}]^\top$. The control reproduction number is $\mathcal{R}_c = \frac{\psi(\sigma_2+\mu_V)}{u\mu_V+\sigma_2\mu_S+\mu_S\mu_V}[\frac{(1+u\theta_2)\alpha}{\varepsilon+\zeta+\lambda+\mu_I} + \frac{(1+u\theta_4)\beta\varepsilon}{(\eta+\rho+\mu_D)(\varepsilon+\zeta+\lambda+\mu_I)} + \frac{(1+u\theta_6)\gamma\zeta}{(\theta+\mu+\kappa+\mu_A)(\varepsilon+\zeta+\lambda+\mu_I)} + \frac{(1+u\theta_8)\delta(\eta\varepsilon\kappa+\eta\varepsilon\mu+\eta\varepsilon\mu_A+\eta\varepsilon\theta+\theta\zeta\eta+\theta\zeta\mu_D+\theta\zeta\rho)}{(\nu+\xi+\tau_1+\mu_R)(\eta+\rho+\mu_D)(\varepsilon+\zeta+\lambda+\mu_I)(\theta+\mu+\kappa+\mu_A)}]$.

III. Optimal Vaccination Control Problem

Problem formulation: We consider an optimal vaccination control problem to minimize both the total fraction of infected and the vaccination effort $u = u(t)$, during the time interval $[0, T]$. The controlled vaccination rate u is contained in matrix G, which we assume is linear in u, i.e., $G = G(u) = G_1 u + G_2$, with $G_i \in \mathbb{R}^{n_2 \times n_2}$. We also assume that u is a Lebesgue measurable function on $[0, T]$, belonging to the admissible set $U_{ad} \doteq \{u \colon u(t) \in K_{ad}\}$, where $K_{ad} = [0, u_{max}]$. The cost functional is

$$J(u, x, w) \doteq \int_0^T \ell(x(t), w(t), u(t)) dt,$$

$$\ell(x(t), w(t), u(t)) \doteq \begin{bmatrix} N^\top & 0 \end{bmatrix} \begin{bmatrix} x(t) \\ w(t) \end{bmatrix} + \alpha_1 u(t)^2 + \alpha_2 u(t), \quad (2)$$

with $\alpha_1 > 0$, $\alpha_2 \geq 0$ and $N \in (0, \infty)^{n_1}$. The cost includes both a quadratic control component, which is the simplest and most common choice in mathematical epidemiology [13], [14] to capture the non-linear increase of the cost at high intervention levels, and a linear control component, which alone may lead to discontinuous optimal profiles, e.g., bang-bang and singular controls [17], but is widely used for its ability to promote sparsity of control variables.

Introducing the control-to-state map $u \mapsto (x(u), w(u))$, we can define the reduced cost $\tilde{J}(u) \doteq J(u, x(u), w(u))$. Then, we look for an optimal control $u^* \in U_{ad}$ such that

$$u^* \in \arg\min_{u \in U_{ad}} \tilde{J}(u) \quad (3)$$

subject to the dynamics (1).

We prove an important property of the cost functional.

Proposition 1: Consider the non-negative cost functional in (2) and let $(u^n)_{n \in \mathbb{N}_0} \subseteq U_{ad}$ be any sequence of admissible controls such that $\tilde{J}_{max} \doteq \sup_{n \in \mathbb{N}_0} \tilde{J}(u^n) < \infty$. Then, there is a subsequence $(u^{n_k})_{n \in \mathbb{N}_0}$ converging weakly to $\tilde{u} \in U_{ad}$. Moreover, $\liminf_{k \to \infty} \tilde{J}(u^{n_k}) \geq \tilde{J}(\tilde{u})$.

Proof: Denote by (x^n, w^n) the solution to (1) with the control u^n. Since $x^n(t) \in [0, \infty)^{n_1}$ $\forall t \geq 0$ and $N \in (0, \infty)^n$, under our assumptions, and with the cost in (2), we have $\|u^n\|^2_{L^2} \leq \alpha_1^{-1} \tilde{J}(u^n) \leq \alpha_1^{-1} \tilde{J}_{max}$. Since $L^2(0, T)$ is a Hilbert space (whence reflexive), by the Banach-Alaoglu theorem [26] there exists a weakly convergent subsequence $(u^{n_k})_{k \in \mathbb{N}_0}$, i.e., there is some $\tilde{u} \in L^2(0, T)$ such that, for all $v \in L^2(0, T)$, $\lim_{k \to \infty} < u^{n_k}, v >= <\tilde{u}, v>$, where $< \cdot, \cdot >$ is the inner product on $L^2(0, T)$. Moreover, by the Banach-Saks theorem [26], $v \in U_{ad}$. Setting $v \equiv \alpha_2$ above, we get (i) $\lim_{k \to \infty} \alpha_2 \|u^{n_k}\|_{L^1} = \alpha_2 \|\tilde{u}\|_{L^1}$. Also, by weak lower-semicontinuity of the norm,

we have (ii) $\liminf_{k\to\infty} \alpha_1 \|u^{n_k}\|_{L^2} \geq \alpha_1 \|\tilde{u}\|_{L^2}$. Finally, since system (1) is smooth and affine in controls, by [27, Section II-H], we get (iii) $\lim_{k\to\infty}(\|x^{n_k} - \tilde{x}\|_{L^\infty} + \|w^{n_k} - \tilde{w}\|_{L^\infty}) = 0$, where $(\tilde{x}, \tilde{w})$ is the solution to (1) corresponding to the control $\tilde{u}$. By combining (i), (ii) and (iii), we obtain $\liminf_{k\to\infty} \tilde{J}(u^{n_k}) \geq \tilde{J}(\tilde{u})$. ∎

Since $\tilde{J}$ is nonnegative, if we take a sequence $(u^n)_{n\in\mathbb{N}_0} \subseteq U_{ad}$ such that $\lim_{n\to\infty} \tilde{J}(u^n) = \inf_{u\in U_{ad}} \tilde{J}(u)$, Proposition 1 shows the existence of an optimal control $u^* \in U_{ad}$, whence (3) is well defined.

Augmented Hamiltonian: We define the Hamiltonian as

$$\mathcal{H}(t, x, w, u, p) \doteq p^\top \begin{bmatrix} (F + bw^\top C)x \\ G(u)w - \operatorname{diag}(Cx)w + Dx + a \end{bmatrix} + \ell(x, w, u), \quad (4)$$

where the co-state $p(t) \doteq [p_x(t)^\top \; p_w(t)^\top]^\top \in \mathbb{R}^{n_1+n_2}$ is the unique solution to the adjoint system

$$-\begin{bmatrix} \dot{p}_x \\ \dot{p}_w \end{bmatrix} = \begin{bmatrix} F + bw^\top C & bx^\top C^\top \\ D - \operatorname{diag}(w)C & G(u) - \operatorname{diag}(Cx) \end{bmatrix}^\top \begin{bmatrix} p_x \\ p_w \end{bmatrix}, \\ + \begin{bmatrix} N \\ 0 \end{bmatrix} \begin{bmatrix} p_x \\ p_w \end{bmatrix}(T) = 0. \quad (5)$$

To shorten the notations, we suppress the dependence on t.

Based on (4), we introduce the augmented Hamiltonian

$$\mathcal{K}_\epsilon(t, x, w, u, p, v) \doteq \mathcal{H}(t, x, w, u, p) + \epsilon(u - v)^2, \quad (6)$$

where $\epsilon > 0$ and $v \in U_{ad}$.

Numerical solution via SQH: We propose to numerically solve our optimal control problem with the sequential quadratic Hamiltonian (SQH) method [19], which is formulated in the framework of the Pontryagin minimum principle and represents an efficient and robust extension of the successive approximations strategy to solve general optimal control problems. The SQH approach, described in Algorithm 1, relies on a sequential point-wise optimization of the augmented Hamiltonian function (6), and generates a sequence of iterates $u^n \in U_{ad}$, where at each step $u^{n+1}(t)$ is obtained by minimizing the augmented Hamiltonian $\mathcal{K}_\epsilon(t, x^n, w^n, v, p^n, u^n)$, where (x^n, w^n) are the solutions to (1) corresponding to the previous iterate u^n.

Since (i) the maps $x \mapsto N^\top x$ and $(x, w) \mapsto f(t, x, w, u) \doteq \begin{bmatrix} (F + bw^\top C)x \\ G(u)w - \operatorname{diag}(Cx)w + Dx + a \end{bmatrix}$ are twice continuously differentiable for every $u \in K_{ad}$ and $t \in [0, T]$, (ii) function f and its first and second derivatives with respect to the state variables x, w are continuous in all their arguments, (iii) the state variables $x(t), w(t)$ are bounded on $t \in [0, T]$, uniformly in $u \in U_{ad}$, and (iv) function f and its first derivatives with respect to the state variables x, w are Lipschitz for $u \in K_{ad}$, uniformly in $t \in [0, T]$ and in (x, w) in the state space, the framework in [21] can be applied to solve the optimal control problem (3) with dynamics (1). Let us define the projection operator $\mathcal{P}_{K_{ad}} : \mathbb{R} \to K_{ad}$ as $\mathcal{P}_{K_{ad}}(\xi) = \min(\max(0, \xi), u_{max})$. First, we show that Algorithm 1 is well-defined.

Proposition 2: Let $u^n \in L^2(0, T)$, $w^n, p^n \in H^1(0, T)$. Then the update u^{n+1} provided by Algorithm 1 is in U_{ad}.

Proof: Recalling (4) and (6) and computing

$$\frac{\partial \mathcal{K}_\epsilon}{\partial u}(t, x^n, w^n, u, p^n, u^n) \\ = (p_w^n)^\top G_1 w^n + 2\alpha_1 u + 2\epsilon(u - u^n) + \alpha_2 = 0,$$

we obtain the following unconstrained minimizer of $\mathcal{K}_\epsilon$:

$$u_{temp}^{n+1} = \frac{\epsilon}{\alpha_1 + \epsilon} u^n - \frac{1}{2(\alpha_1 + \epsilon)} (p_w^n)^\top G_1 w^n - \frac{\alpha_2}{2(\alpha_1 + \epsilon)}. \quad (7)$$

From the measurability of u^n, w^n, p^n it follows the measurability of $u^{n+1}(t) = \mathcal{P}_{K_{ad}}(u_{temp}^{n+1}(t))$. Since $u^{n+1}(t) \in [0, u_{max}]$, we obtain that $u^{n+1} \in U_{ad}$. ∎

Algorithm 1 SQH Method

1: Choose $\epsilon > 0$, $\bar{\tau} > 0$, $\omega > 1$, $\phi \in (0, 1)$, $\chi \in (0, \infty)$ and initial guess u^0; compute x^0, w^0, p^0; set $n = 0$.
2: Solve $\tilde{u}(t) = \arg\min_{v\in K_{ad}} \mathcal{K}_\epsilon(t, x^n, w^n, v, p^n, u^n)$ for all $t \in [0, T]$.
3: Compute $\tilde{x}, \tilde{w}$ corresponding to $\tilde{u}$, and $\tau \doteq \|\tilde{u} - u^n\|_{L^2}^2$.
4: IF $J(\tilde{u}, \tilde{x}) - J(u^n, x^n) \leq -\chi\tau$, THEN assign $\epsilon \leftarrow \phi\epsilon$, $x^{n+1} \leftarrow \tilde{x}$, $w^{n+1} \leftarrow \tilde{w}$, $u^{n+1} \leftarrow \tilde{u}$; compute p^{n+1} corresponding to x^{n+1}, w^{n+1} and u^{n+1}. Set $n \leftarrow n + 1$. ELSE: keep x^n, w^n and u^n, and assign $\epsilon \leftarrow \omega\epsilon$.
5: IF $\tau < \bar{\tau}$, THEN STOP and return u^n. ELSE go to 2.

Note that for the sequence of iterates $(u^n)_{n\in\mathbb{N}_0} \subseteq U_{ad}$ in Algorithm 1, the sequence $(\tilde{J}(u^n))_{n\in\mathbb{N}_0}$ is non-negative and non-increasing. Hence, Proposition 1 implies that $(u^n)_{n\in\mathbb{N}_0}$ has a weak accumulation point $\tilde{u}$ in U_{ad}.

We now show that, for our considered class of problems, any strong accumulation point $\tilde{u}$ of the SQH method satisfies the first-order optimality conditions. For this purpose, as in [21], we prove the following result.

Proposition 3: There exists some $r > 0$ such that, for any iterate u^n, $n \in \mathbb{N}_0$, and for any $\epsilon > 0$ in Algorithm 1,

$$\mathcal{K}_\epsilon(t, x^n, w^n, z, p^n, u^n) - \mathcal{K}_\epsilon\left(t, x^n, w^n, u^{n+1}, p^n, u^n\right) \\ \geq r\left(z - u^{n+1}\right)^2, \quad (8)$$

for all $z \in K_{ad} \subseteq [0, \infty)$ and for all $t \in [0, T]$.

Proof: Assume that $u_{temp}^{n+1} \in (0, u_{max})$, whence $u^{n+1} = u_{temp}^{n+1}$. Given $z \in K_{ad}$, we have

$$\mathcal{K}_\epsilon\left(t, x^n, w^n, z, p^n, u^n\right) - \mathcal{K}_\epsilon\left(t, x^n, w^n, u^{n+1}, p^n, u^n\right) \\ = \left(z - u^{n+1}\right)(p_w^n)^\top G_1 w^n + (\alpha_1 + \epsilon)\left(z - u^{n+1}\right)\left(z + u^{n+1}\right) \\ - 2\left(z - u^{n+1}\right)\epsilon u^n + \alpha_2\left(z - u^{n+1}\right) \\ = (\alpha_1 + \epsilon)\left(z - u^{n+1}\right)^2,$$

where the second equality is obtained by substituting $\epsilon u^n = (\alpha_1 + \epsilon)u^{n+1} + \alpha_2/2 + (p_w^n)^\top G_1 w^n/2$ from (7) and performing algebraic manipulations. Hence, (8) holds with $r = \alpha_1$. Next, assume that $u_{temp}^{n+1} \leq 0$, whence $u^{n+1} = 0$. Then, since $\mathbb{R} \ni u^{n+1} \mapsto \mathcal{K}_\epsilon(t, x^n, w^n, u^{n+1}, p^n, u^n)$ is quadratic, it must hold that

$$\frac{\partial \mathcal{K}_\epsilon}{\partial u^{n+1}}(t, x^n, w^n, 0, p^n, u^n) = (p_w^n)^\top G_1 w^n - 2\epsilon u^n + \alpha_2 \geq 0.$$

Therefore, for $z \in K_{ad}$,

$$\mathcal{K}_\epsilon\left(t, x^n, w^n, z, p^n, u^n\right) - \mathcal{K}_\epsilon\left(t, x^n, w^n, 0, p^n, u^n\right) \\ = z\left[(p_w^n)^\top G_1 w^n - 2\epsilon u^n + \alpha_2\right] + (\alpha_1 + \epsilon)z^2 \geq \alpha_1 z^2,$$

and again (8) holds with $r = \alpha_1$. Finally, assume that $u^{n+1}_{temp} \geq u_{max}$, whence $u^{n+1} = u_{max}$. Then, it must hold that

$$\frac{\partial \mathcal{K}_\epsilon}{\partial u^{n+1}}\left(t, x^n, w^n, u_{max}, p^n, u^n\right) = \left(p^n_w\right)^\top G_1 w^n + 2(\alpha_1 + \epsilon)u_{max} - 2\epsilon u^n + \alpha_2 \leq 0,$$

whence $(p^n_w)^\top G_1 w^n - 2\epsilon u^n \leq -2(\alpha_1+\epsilon)u_{max} - \alpha_2$. Therefore, for $z \in K_{ad}$, since $z - u_{max} \leq 0$,

$$\begin{aligned}&\mathcal{K}_\epsilon\left(t, x^n, w^n, z, p^n, u^n\right) - \mathcal{K}_\epsilon\left(t, x^n, w^n, u_{max}, p^n, u^n\right)\\ &= (z - u_{max})\left\{\left[\left(p^n_w\right)^\top G_1 w^n - 2\epsilon u^n\right] + (\alpha_1 + \epsilon)(z + u_{max}) + \alpha_2\right\}\\ &\geq (\alpha_1 + \epsilon)(z - u_{max})^2,\end{aligned}$$

and once again (8) holds with $r = \alpha_1$. ∎

Then, our main result follows from Proposition 3 and [21][Theorem 3.1].

Theorem 1: Consider the optimal control problem (3) subject to the dynamics (1) and let the sequence $(u^n)_{n\in\mathbb{N}_0}$ be generated by Algorithm 1, Steps 2-4. Then, for any subsequence $(u^k)_{k\in K}$, $K \subseteq \mathbb{N}_0$, such that $\lim_{k\to\infty} u^k(t) = \tilde{u}(t)$ for almost all $t \in (0, T)$, it holds that $\tilde{u} \in U_{ad}$ and $\mathcal{H}(t, \tilde{x}, \tilde{w}, \tilde{u}, \tilde{p}) = \min_{z\in K_{ad}} \mathcal{H}(t, \tilde{x}, \tilde{w}, z, \tilde{p})$ for almost all $t \in (0, T)$, where $\tilde{x}, \tilde{w}$ solve (1) with the control $\tilde{u}$ and $\tilde{p}$ is the corresponding co-state solving (5) for $\tilde{x}, \tilde{w}$ and $\tilde{u}$.

Remark 1: In fact, by [21, Corollary 3.1], it follows that for any $\varsigma > 0$ and $\varphi \in (0, T)$, there exists some $N \in \mathbb{N}$ for which u^N is (ς, φ)-suboptimal, i.e., $\mathcal{H}(t, x^N, w^N, u^N, p^N) \leq \mathcal{H}(t, x^N, w^N, z, p^N) + \varsigma$ holds for all $z \in K_{ab}$, a.e. outside a set in $(0, T)$ of measure less than φ.

IV. The SQH Approach to Vaccination Control

We perform thorough numerical experiments by solving the optimal vaccination control problem (3), subject to the dynamics of the extended SIDARTHE-V model in Example 1, with the SQH scheme. We also compare the performance of SQH and FBS [12], [23].

In the full version that is available online [25], we also consider numerical simulations for an extended SIRV and an extended SEIRV model, along with a sensitivity analysis.

A. Extended SIDARTHE-V: Optimal Vaccination Control

For the extended SIDARTHE-V model, the running cost in (2) becomes $\ell(x(t), w(t), u(t)) \doteq \eta_1 I + \eta_2 D + \eta_3 A + \eta_4 R + \eta_5 T + \alpha_1 u(t)^2 + \alpha_2 u(t)$, where $\eta_i > 0$ for $i = 1, 2, 3, 4, 5$, $\alpha_1 > 0$ and $\alpha_2 \geq 0$.

Given the parameter values in Fig. 1, the threshold u_{thr} such that $\mathcal{R}_c < 1$ if $u > u_{thr}$ can be computed analytically from the expression of $\mathcal{R}_c$ in Example 1. Since any control satisfying $\inf_{t\in[0,T]} u(t) > 3.5 \cdot 10^{-3}$ ensures $\mathcal{R}_c < 1$, we choose $u_{max} = 0.1 > u_{thr}$ for our simulations, so as to guarantee that the control objective is feasible.

We first conduct a comparative analysis between the SQH and the FBS methods, with a horizon of $T = 350$ days, while varying the weight selections within the cost functional. The FBS procedure is applied until either convergence or a maximum iteration limit (set at 10000 iterations) is reached. Thus, the absence of convergence indicates the exhaustion of the maximum iteration count. With $\eta_i = 10^3$ for all i, $\alpha_1 = 1$ and $\alpha_2 = 0$, both methods converge; FBS requires 1.03 s of CPU time, while SQH only takes 0.74 s (however, SQH is much faster than FBS, by a factor of 20, when other numerical examples are considered, see [25]). Fig. 1 shows the solutions obtained by both methods, which are in agreement, and also captures the system evolution in the absence of a control policy, showcasing how the implementation of vaccination reduces the peak of infectiousness across all infected compartments, and significantly reduces deaths, by one order of magnitude, in the considered horizon.

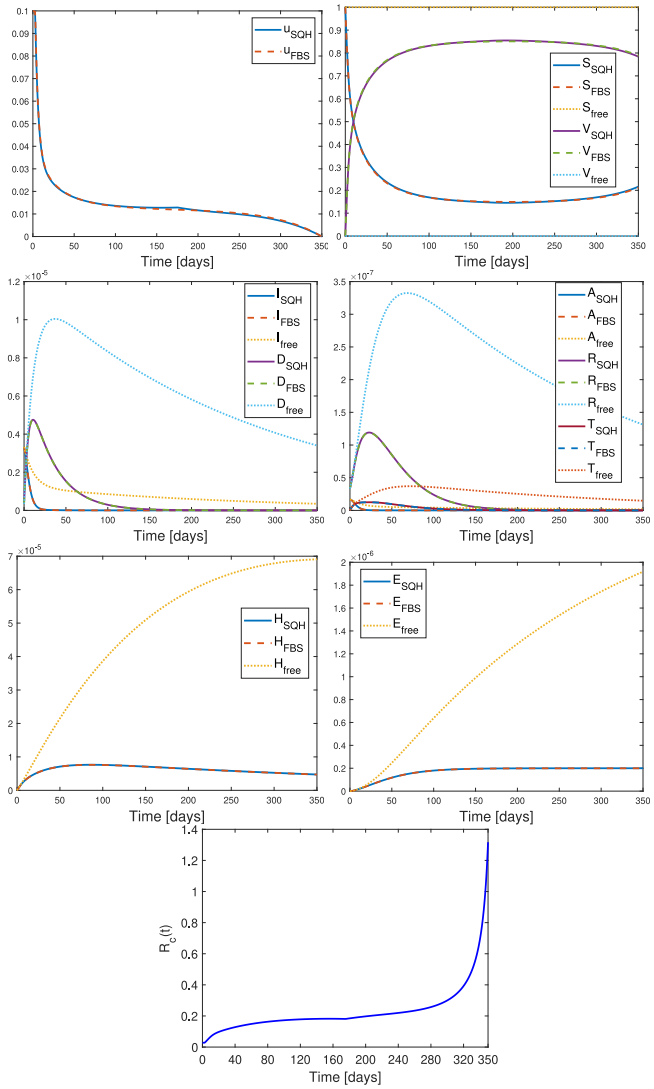

Fig. 1. Optimal vaccination with SIDARTHE-V dynamics, with parameters $\alpha = 0.3567$, $\beta = 0.0053$, $\gamma = 0.1485$, $\delta = 0.005$, $\epsilon = 0.2988$, $\zeta = 0.0025$, $\lambda = 0.1128$, $\eta = 0.0015$, $\rho = 0.032$, $\theta = 0.37$, $\mu = 0.12$, $\kappa = 0.02$, $\tau_1 = 0.005$, $\tau_2 = 0.17$, $\nu = 0.02$, $\xi = 0.022$, $\sigma = 0.024$ [9]; $\sigma_1 = 1/500$, $\sigma_2 = 1/500$, $\psi = 2.91 \cdot 10^{-5}$, $\mu_I = 6.25 \cdot 10^{-4}$ and $\mu_j = 2.9 \cdot 10^{-5}$ for $j \neq I$ [10], [11]; $\theta_1 = 0.0013$, $\theta_2 = 0.0021$ [28]. Initial conditions are $I_0 = 10^{-6}$, $D_0 = A_0 = R_0 = T_0 = H_0 = E_0 = V_0 = 0$, $S_0 = 1 - I_0$. Optimal vaccination rate and system dynamics at optimality with FBS (dashed) and SQH (solid); uncontrolled dynamics (dotted). The cost weights are $\eta_i = 10^3$, $\alpha_1 = 1$ and $\alpha_2 = 0$. The evolution of $\mathcal{R}_c$ remains below the critical value 1 until vaccination ceases.

If the L^2 weight is reduced to $\alpha_1 = 0.1$, the control effort increases, reaching u_{max} in the first days, and the number of infected and deceased is further reduced, as shown in Fig. 2. Both methods converge to the same solution, SQH in 0.98 s (6 iterations) and FBS in 1.13 s (10 iterations).

With $\eta_i = 10^3$ for all i and $\alpha_1 = 1$, we now consider the L^1 control term with weight (i) $\alpha_2 = 0.1$, (ii) $\alpha_2 = 0.3$, and (iii)

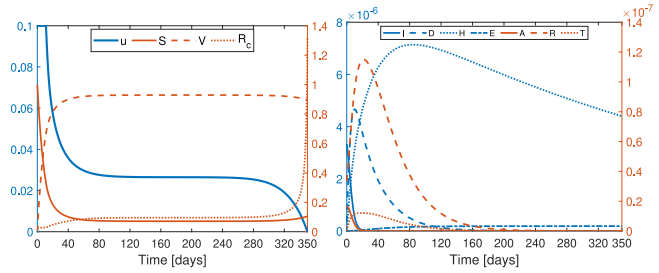

Fig. 2. Optimal vaccination with SIDARTHE-V dynamics (parameters as in Fig. 1) and cost functional weights $\eta_i = 10^3$, $\alpha_1 = 0.1$, $\alpha_2 = 0$. The optimal vaccination profile and the system evolution are shown alongside the evolution of $\mathcal{R}_c$.

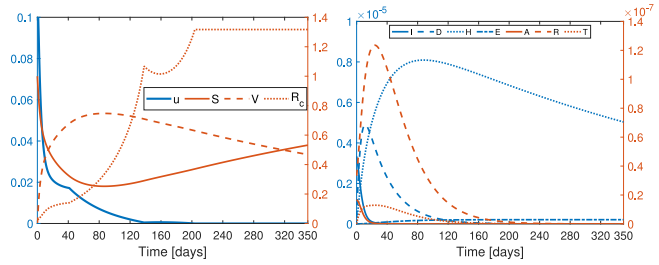

Fig. 3. Optimal vaccination with SIDARTHE-V dynamics (parameters as in Fig. 1) and cost functional weights $\eta_i = 10^3$, $\alpha_1 = 1$, $\alpha_2 = 0.1$. The optimal vaccination profile and the system evolution are shown alongside the evolution of $\mathcal{R}_c$.

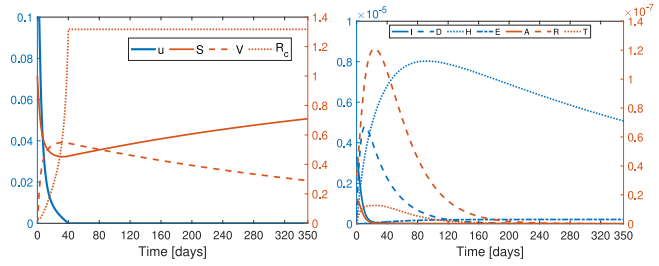

Fig. 4. Optimal vaccination with SIDARTHE-V dynamics (parameters as in Fig. 1) and cost functional weights $\eta_i = 10^3$, $\alpha_1 = 1$, $\alpha_2 = 0.3$. The optimal vaccination profile and the system evolution are shown alongside the evolution of $\mathcal{R}_c$.

$\alpha_2 = 1$. In all these cases, FBS fails to converge after 10000 iterations, while SQH achieves convergence within 1.21 s (20 iterations), providing the results shown in Fig. 3, Fig. 4 and Fig. 5, respectively. Increasing α_2 leads to a sparser control, which causes more infections and deaths, as $\mathcal{R}_c > 1$ for most of the horizon; for $\alpha_2 = 1$, we obtain a bang-bang control with switching time after approximately 5 days.

Optimal vaccination control with non-smooth cost: To further showcase the potential of the SQH method, we consider an optimal vaccination problem with a non-smooth term, which cannot be handled by FBS. For our case study, we consider the extended SIDARTHE-V model with the same parameter values as before, and the running cost

$$\ell_1(x(t), w(t), u(t)) \doteq \ell(x(t), w(t), u(t)) + \alpha_3 g(u),$$

with $\alpha_3 > 0$ and

$$g(u) = \begin{cases} |u - \bar{u}| & \text{if } |u - \bar{u}| > \bar{s} \\ 0 & \text{otherwise} \end{cases}$$

where $\bar{s}$ is a given threshold and $\bar{u}$ is a desired piecewise-constant vaccination profile. We consider a profile $\bar{u}$ that

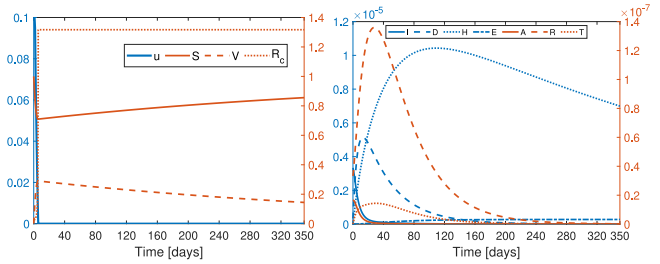

Fig. 5. Optimal vaccination with SIDARTHE-V dynamics (parameters as in Fig. 1) and cost functional weights $\eta_i = 10^3$, $\alpha_1 = 1$, $\alpha_2 = 1$. The optimal vaccination profile and the system evolution are shown alongside the evolution of $\mathcal{R}_c$.

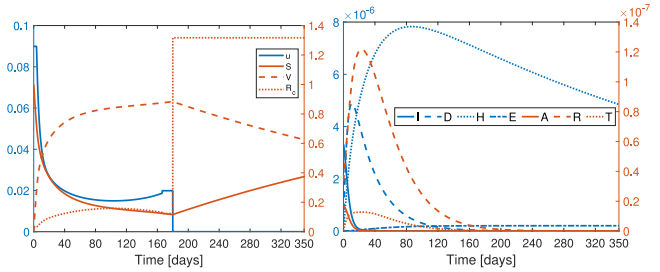

Fig. 6. Optimal vaccination with SIDARTHE-V dynamics (parameters as in Fig. 1) and non-smooth cost functional with weights $\eta_i = 10^3$, $\alpha_1 = 1$, $\alpha_2 = 1$, $\alpha_3 = 1$. The optimal vaccination profile and the system evolution are shown alongside the evolution of $\mathcal{R}_c$.

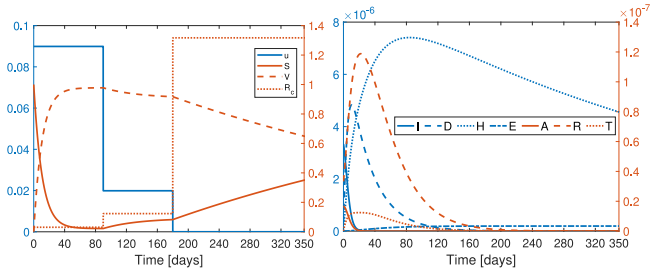

Fig. 7. Optimal vaccination with SIDARTHE-V dynamics (parameters as in Fig. 1) and non-smooth cost functional with weights $\eta_i = 10^3$, $\alpha_1 = 1$, $\alpha_2 = 1$, $\alpha_3 = 10$. The optimal vaccination profile and the system evolution are shown alongside the evolution of $\mathcal{R}_c$.

divides the time horizon $T = 350$ (approximately one year) into four seasons, starting from autumn. A flu vaccine is usually highly recommended at the beginning of the autumn, also administered during the winter, but typically not administered during spring and summer. Thus, we set

$$\bar{u}(t) = \begin{cases} 0.09 & \text{if } t \in [0, T/4] \\ 0.02 & \text{if } t \in (T/4, T/2] \\ 0 & \text{if } t \in [T/2, T] \end{cases}$$

Also, we set $\bar{s} = 10^{-4}$. The parameter values are the same as those in Fig. 1. The cost functional weights $\eta_i = 10^3$ for all i, $\alpha_1 = 1$, $\alpha_2 = 1$, $\alpha_3 = 1$ lead to the results in Fig. 6: the obtained optimal control tries to track $\bar{u}$ as much as possible, but the other cost components prevail. If we increase the weight to $\alpha_3 = 10$, the optimal vaccination rate adheres to the desired profile $\bar{u}$, as shown in Fig. 7. For a comparison, Fig. 5 shows the optimal solution without the non-smooth term, showing its significant effect on the vaccination campaign.

V. Concluding Discussion

We have introduced a general class of mathematical models describing disease spreading dynamics through an arbitrary number of infected and non-infected compartments, and formulated the related optimal control problem for vaccination planning. To numerically solve the problem, we have adopted the recently proposed SQH method [19], [20], [21], [22], for the first time in an epidemiological context, and we have proved rigorous global convergence guarantees. A vast campaign of numerical experiments (see also [25]) has successfully validated our theoretical results.

Thanks to its ability to handle complex large-scale models and its straightforward implementation (based on a similar concept to that of FBS [12]), SQH enjoys the same scalability and simplicity of implementation that make FBS the algorithm of choice for optimal control in systems biology and epidemiology [23]. However, we have shown that SQH surpasses FBS in numerical performance: it converges faster, it converges even when FBS does not, and, unlike FBS, it is applicable even when handling non-smooth cost functionals. Most importantly, we have demonstrated rigorous global convergence guarantees for the SQH method for any initialization, which hold, in the case of smooth cost functionals, for a very general class of (epidemiological) systems. The existence of such convergence guarantees is of primary importance, while their lack is a fundamental limitation of the FBS method. In fact, FBS suffers from numerous challenges, as evidenced in [23], [24]. Its convergence rate (and even lack of convergence) poses a significant numerical issue, only partially mitigated by incorporating acceleration methods [23], while theoretical guarantees for FBS are limited to *local* convergence to a controller-state trajectory pair (u_*, x_*) that satisfies first-order optimality conditions. Hence, the initial guess of the controller-state pair needs to be sufficiently close to (u_*, x_*), but no explicit bounds on the required proximity are available in the literature [24]. Not only the convergence of FBS is not guaranteed in general and is influenced by the choice of the initial guess, but also, as demonstrated in [24, Remark 4.1], even a minor change in the parameter values of a toy model may lead to an optimal control problem for which FBS does not converge at all.

In view of its generality, straightforward implementation, theoretical convergence guarantees for smooth cost functions, and improved numerical performance with respect to the state of the art, including the possibility to handle non-smooth cost functions, we believe that our proposed method has the potential to become a benchmark for optimal control in systems biology and mathematical epidemiology.

Acknowledgment

Work funded by the European Union. Views and opinions expressed are however those of the authors only and do not necessarily reflect those of the EU, the European Research Executive Agency or the European Research Council. Neither the EU nor the granting authority can be held responsible for them.

References

[1] O. Diekmann and J. A. P. Heesterbeek, *Mathematical Epidemiology of Infectious Diseases: Model Building, Analysis and Interpretation*. Hoboken, NJ, USA: Wiley, 2000.

[2] H. W. Hethcote, "The mathematics of infectious diseases," *SIAM Rev.*, vol. 42, no. 2, pp. 599–653, 2000.

[3] F. Brauer and C. Castillo-Chavez, *Mathematical Models in Population Biology and Epidemiology*, 2nd ed. New York, NY, USA: Springer, 2012.

[4] T. Alamo, D. G. Reina, P. M. Gata, V. M. Preciado, and G. Giordano, "Data-driven methods for present and future pandemics: Monitoring, modelling and managing," *Ann. Rev. Control*, vol. 52, pp. 448–464, Dec. 2021.

[5] E. Hernandez-Vargas, A. González, C. Beck, X. Bi, F. Calà Campana, and G. Giordano, "Modelling and control of epidemics across scales," in *Proc. IEEE Conf. Decision Control (CDC)*, 2022, pp. 4963–4980.

[6] W. Kermack and A. McKendrick, "A contribution to the mathematical theory of epidemics," *Proc. Roy. Soc. London*, vol. 115, no. 772, pp. 700–721, 1927.

[7] A. B. Gumel et al., "Modelling strategies for controlling SARS outbreaks," *Proc. R. Soc. B, Biol. Sci.*, vol. 271, no. 1554, pp. 2223–32, 2004.

[8] G. Giordano et al., "Modelling the COVID-19 epidemic and implementation of population-wide interventions in Italy," *Nat. Med.*, vol. 26, pp. 855–860, Apr. 2020.

[9] G. Giordano et al., "Modeling vaccination rollouts, SARS-CoV-2 variants and the requirement for non-pharmaceutical interventions in Italy," *Nat. Med.*, vol. 27, pp. 993–998, Apr. 2021.

[10] B. Buonomo, R. Della Marca, A. d'Onofrio, and M. Groppi, "A behavioural modelling approach to assess the impact of COVID-19 vaccine hesitancy," *J. Theor. Biol.*, vol. 534, Feb. 2022, Art. no. 110973.

[11] T. Krueger et al., "Risk assessment of COVID-19 epidemic resurgence in relation to SARS-CoV-2 variants and vaccination passes," *Commun. Med.*, vol. 2, p. 23, Mar. 2022.

[12] S. Lenhart and J. T. Workman, *Optimal Control Applied to Biological Models*. Atlanta, GA, USA: Chapman Hall, 2007.

[13] O. Sharomi and T. Malik, "Optimal control in epidemiology," *Ann. Oper. Res.*, vol. 251, pp. 55–71, Apr. 2017.

[14] B. Buonomo, P. Manfredi, and A. d'Onofrio, "Optimal time-profiles of public health intervention to shape voluntary vaccination for childhood diseases," *J. Math. Biol.*, vol. 78, pp. 1089–1113, Mar. 2019.

[15] J. Köhler, L. Schwenkel, A. Koch, J. Berberich, P. Pauli, and F. Allgöwer, "Robust and optimal predictive control of the COVID-19 outbreak," *Ann. Rev. Control*, vol. 51, pp. 525–539, Jun. 2021.

[16] F. Blanchini, P. Bolzern, P. Colaneri, G. D. Nicolao, and G. Giordano, "Generalized epidemiological compartmental models: Guaranteed bounds via optimal control," in *Proc. IEEE Conf. Dec. Control (CDC)*, 2021, pp. 3532–3537.

[17] L. Freddi, "Optimal control of the transmission rate in compartmental epidemics," *Math. Control Relat. Fields*, vol. 12, no. 1, pp. 201–223, 2022.

[18] J. Arino, F. Brauer, P. van den Driessche, J. Watmough, and J. Wu, "A final size relation for epidemic models," *Math. Biosc. Eng.*, vol. 4, no. 2, p. 159, 2007.

[19] A. Borzì, *The Sequential Quadratic Hamiltonian Method: Solving Optimal Control Problems*. Atlanta, GA, USA: Chapman Hall, 2023.

[20] T. Breitenbach, "A sequential quadratic hamiltonian scheme for solving optimal control problems with non-smooth cost functionals," Ph.D. dissertation, Dept. Math., Univ. Würzburg, Würzburg, Germany, 2019.

[21] T. Breitenbach and A. Borzì, "A sequential quadratic hamiltonian scheme for solving non-smooth quantum control problems with sparsity," *J. Comput. Appl. Math.*, vol. 369, May 2020, Art. no. 112583.

[22] F. Calà Campana and A. Borzì, "On the SQH method for solving differential Nash games," *J. Dyn. Control Syst.*, vol. 28, pp. 739–755, Oct. 2022.

[23] J. A. Sharp, K. Burrage, and M. J. Simpson, "Implementation and acceleration of optimal control for systems biology," *J. Roy. Soc. Interface*, vol. 18, no. 181, 2021, Art. no. 20210241.

[24] M. McAsey, L. Mou, and W. Han, "Convergence of the forward-backward sweep method in optimal control," *Comput. Optim. Appl.*, vol. 53, pp. 207–226, Sep. 2012.

[25] F. Calà Campana, R. Katz, and G. Giordano. "Sequential-quadratic-hamiltonian optimal control of epidemic models with an arbitrary number of infected and non-infected compartments." 2024. [Online]. Available: https://giuliagiordano.dii.unitn.it/docs/SQHepid2024.pdf

[26] R. E. Megginson, *An Introduction to Banach Space Theory* (Graduate texts in Mathematics), vol. 183, New York, NY, USA: Springer, 2012.

[27] E. D. Sontag, *Mathematical Control Theory: Deterministic Finite Dimensional Systems* (Texts in Applied Mathematics), vol. 6, New York, NY, USA: Springer, 2013.

[28] V. Hall et al., "Protection against SARS-CoV-2 after COVID-19 vaccination and previous infection," *New Eng. J. Med.*, vol. 386, no. 13, pp. 1207–1220, 2022.

Open Access funding provided by "Università degli Studi di Trento" within the CRUI CARE Agreement